Transceiver Grouping: A Novel Diversity Method for Collaborative Multiuser FSO Communications

Chadi Abou-Rjeily, *Senior Member IEEE*

***Abstract*—In this paper, we propose a novel multipoint-to-multipoint cooperative diversity scheme for multiuser Free-Space Optical (FSO) communications. This scheme is motivated by the inherit immobility and directivity of FSO communications where several transceivers mounted on a given building can be easily interconnected for achieving enhanced diversity levels through joint encoding/decoding. In this case, the N users are clustered in a number of groups depending on the state of the FSO network. Users of a given group transmit the same encoded symbol comprising the information of all these users while Maximum-Ratio Combining (MRC) is implemented at the receive apertures. We present an asymptotic analysis of the bit error rate and derive the achievable diversity orders over the gamma-gamma turbulence-induced fading channels affected by pointing errors. Results show that while grouping all users in one group achieves the highest diversity order, this partitioning is suboptimal for practical ranges of the Signal-to-Noise Ratio (SNR). In this context, the partitioning of the N users turns out to be of crucial importance where the optimal grouping outperforms the all-user grouping by several orders of magnitude.**

***Index Terms*—Free-Space Optics (FSO), cooperation, diversity, performance analysis, gamma-gamma, order statistics, partitioning, Maximum Ratio Combining (MRC).**

I. Introduction

Atmospheric turbulence, or scintillation, constitutes one of the major sources of nuisance for Free-Space Optical (FSO) communications [1], [2]. This renders fading-mitigation techniques inevitable for future FSO networks in order to attain reliable high data-rate communications. These techniques include the collocated Multiple-Input-Multiple-Output (MIMO) methods as well as the distributed cooperative diversity solutions. Cooperative communications benefit from the presence of multiple communicating nodes in the network for realizing spatial diversity gains by diversifying the paths along which the information-carrying light signals propagate.

The vast majority of the investigated cooperative diversity methods corresponds to the point-to-point cooperative schemes also referred to as the relaying techniques where a number of neighboring communicating nodes serve as relays for the sake of assisting a source node S in its communication with a destination node D. The point-to-point cooperative schemes include serial relaying and parallel relaying. In the case of serial relaying, the signal is retransmitted sequentially from one relay to another until it reaches D [3], [4]. On the other hand, parallel relaying typically involves the two source-relays and relays-destination communication phases [5]–[12]. For both relaying schemes, either the Amplify-and-Forward (AF) [5]–[7] or the Decode-and-Forward (DF) [5], [8]–[10] retransmission strategies can be envisaged. In a similar way, either the totality of the relays or a subset of these relays can participate in the cooperation effort depending on the availability of the Channel State Information (CSI) where these two variants are referred to as all-active relaying [5]–[10] and selective relaying [11], [12], respectively. More recent solutions include inter-relay cooperation where the relays exchange information with each other before the transmission phase to the destination [13], [14].

The point-to-point solutions in [3]–[14] present a number of limitations that vary depending on the role played by the relay nodes. In fact, the relays in a cooperative network can correspond either to independent entities that have their own information to communicate or to dedicated entities that are added with the mere objective of assisting S in its communication with D. The main implication of the first scenario resides in the fact that a relay can assist S only if it has no information to transmit during a certain communication session. In other words, the relays are not available on demand and their availability will drop within the peak times during which cooperative transmissions are much needed. Consequently, this solution seems to be more adapted to Radio-Frequency (RF) wireless systems with Time Division Multiple Access (TDMA) rather than FSO systems where all nodes in the network can transmit simultaneously without suffering from interference following from the high directivity of the FSO links. In the former case, the retransmissions from the relay (that are dedicated for assisting the source) will occur in the source's time slot while the relay will proceed with the transmission of its own information in its own dedicated time slot. This cooperation scheme is known to be spectrally efficient for TDMA-RF systems and the relay can uninterruptedly assist the source by switching its transmissions during the different TDMA slots [15]. On the other hand, the second scenario is not cost-effective because of the infrastructure that needs to be added while taking into account a number of geographic constraints [16].

In addition to the point-to-point cooperative FSO systems, Multiuser Diversity (MD) FSO systems were considered in [17]–[22]. The system model that is adopted in these references corresponds to a point-to-multipoint scenario where a central node is equipped with K apertures each dedicated to communicating with one of the K users. In this case, each one of the K apertures at the central node is directed to a certain user where only one of these apertures is active in each time slot. In [17], a number of scheduling schemes were

The author is with the Department of Electrical and Computer Engineering of the Lebanese American University (LAU), Byblos, Lebanon. (e-mail: chadi.abourjeily@lau.edu.lb).

compared in terms of the achievable levels of compromise between throughput and latency where at a given time instant the cental node serves the user with the largest channel gain. This MD system was extended in [18], [19] to the more general selection scheme where the N-th best user is selected. In [18] the outage probability, bit error rate, average capacity and diversity order were derived over lognormal and gamma-gamma fading channels while [19] targeted the bit error rate and average capacity over the exponentiated Weibull channels. The select-max MD scheduling scheme was analyzed in [20] where closed form outage-capacity expressions were derived under the assumption of lognormal channels. While the MD scheduling systems in [17]–[20] are based on Single-Input-Single-Output (SISO) FSO links, [21] considered the extension to the case of MIMO links. In this reference, the round robin, opportunistic round Robin, select-max and N-th best user selection scheduling protocols were compared over lognormal channels.

The point-to-point [3]–[14] and point-to-multipoint [17]–[22] FSO systems are often inspired from RF communications where we can find the counterparts of these schemes in the literature on RF wireless communications. In this context, communicating over FSO channels presents a number of particularities that clearly distinguish FSO systems from RF systems rendering the design of FSO-specific schemes a viable option that is worth investigating where the additional degrees of freedom can lead to novel designs that combine simplicity and efficiency. First, FSO transceivers are static unlike the mobile nodes in a RF network. Secondly, FSO links are highly directive unlike the broadcast nature of RF transmissions. These two differentiating factors and the observation that several FSO transceiver pairs might be present on two buildings led to the multipoint-to-multipoint FSO-specific cooperative scheme that we propose in this work. While latency is a critical issue in the MD scheduling schemes [17]–[22], the proposed solution does not introduce any latency where any user can access the channel at any time.

Consider the case of N FSO transceiver pairs mounted on two buildings for the sake of establishing N FSO links between the premises of N different enterprisers denoted by users. The proposed scheme is based on connecting the transceivers installed in the same building by means of wires following from the geographic vicinity and immobility of these transceivers. Based on this connection, instead of having each user transmitting its own data as in noncooperative systems, a user can now partner with other users to generate a jointly encoded symbol that is then transmitted over the FSO links of this group of users. This form of repetition coding is capable of achieving diversity in the absence of interference. At the receiver side, Maximum-Ratio Combining (MRC) is applied on the received signals for the sake of maximizing the received Signal-to-Noise Ratio (SNR). We evaluate the bit error rate of the proposed scheme over gamma-gamma turbulence-induced fading channels affected by pointing errors. The analytical framework involves the approximation of the probability density function (pdf) of the sum of n order statistics ($1 \leq n \leq N$) and is useful for deriving the achievable diversity orders. The proposed scheme calls for partitioning the N users in a number of groups depending on the state of the FSO network. The developed mathematical analysis guides the partitioning of the N users and excludes numerous partitions that are always outperformed by other partitions.

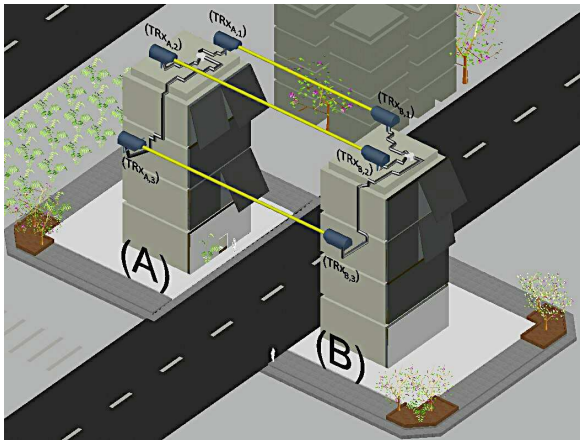

Fig. 1. The proposed cooperative FSO system.

It is worth noting that the proposed multipoint-to-multipoint scheme differs substantially from the MIMO FSO schemes [23], [24]. The main difference resides in the fact that the considered scheme is a multiuser scheme where the information from N users must be accommodated whereas the MIMO schemes involve the communication of the information of a single user through multiple apertures. In this context, aperture grouping is not a concern in MIMO systems where the optimal solution corresponds to activating all apertures [23] and the strongest aperture [24] in the absence and presence of CSI, respectively. On the other hand, for the proposed MD scheme, the user grouping is of critical importance and the optimal grouping strategy depends on the number of users. Finally, for MIMO systems, the apertures are placed within the same FSO transceiver and are hence very close to each other (order of centimeters) implying that the signal transmitted by one transmit aperture will be detected by all receive apertures. This is not the case for MD schemes where the different FSO transmitters and receivers are separated by several meters and hence the optical links of the different users do not interfere with each other.

On the other hand, the proposed solution can not be perceived as an alternative to relay-assisted systems. While serial and parallel relaying are inevitable to extend the network coverage, the proposed scheme results in enhanced performance levels for a given communication distance. In this context, this scheme can complement relay-assisted networks by boosting the reliability of the established S-D, S-R and R-D links.

II. System Model

A. Cooperation Strategy

The proposed cooperation strategy is illustrated in Fig. 1. FSO transceivers are mounted on building rooftops or under windows in order to realize optical wireless connectivity between two distant locations. The FSO connections are highly directive and a distinct pair of perfectly aligned FSO

transceivers is dedicated to each optical link over which a user communicates its information. The key observation is that several optical links might exist between two buildings where each one of these links corresponds to a different user. The potential presence of several neighboring transceivers on each building motivates the multiuser cooperation scheme that we propose in this paper. The main idea is to connect transceivers of the same building by wires that ensure the availability of the information of one user to the other users[1]. This renders joint encoding/decoding possible and allows to develop an FSO-specific fading-mitigation solution by diversifying the links along which the information signals of each user propagate.

It is worth noting that the proposed scheme constitutes a cost-effective solution that is intended to work with the existing infrastructure. In other words, in the case where multiple links already exist between two buildings, then the proposed scheme takes advantage from the presence of these links to boost the reliability of all concerned users. In this context, no extra FSO units are added and the different users simply share their existing resources (per-installed FSO units) in a more efficient way. In other words, the initially established FSO links, that were designed and deployed to operate in a conventional noncooperative manner, will be utilized for cooperative transmissions. A natural choice for the deployment of wireless networks is to avoid the interference between the communicating users. In FSO systems, this condition can be easily satisfied given the high directivity of the laser beams implying that a reasonable separation of the transceivers is sufficient for decoupling the optical links and, in most scenarios, the optical spot at the receiver does not exceed the physical dimensions of the transceiver.

Consider the case of N FSO links connecting sites in buildings (A) and (B). Denote by $\text{TRx}_{\text{X},n}$ the n-th user transceiver on building X. The proposed scheme is based on the following strategy. (i): The N users are first partitioned into the subsets $\mathcal{S}_1, \mathcal{S}_2, \ldots$ based on the CSI. (ii): For the transmission of the information from users in $\mathcal{S}_i$, a symbol comprising the information from all of these users is generated. (iii): The generated symbol is transmitted over the $|\mathcal{S}_i|$ links $\text{TRx}_{\text{A},n}$-$\text{TRx}_{\text{B},n}$ for $n \in \mathcal{S}_i$. (iv): MRC is performed on the signals received at the transceivers $\{\text{TRx}_{\text{B},n}\}_{n\in\mathcal{S}_i}$ that are connected by wires and a decision is made on the transmitted symbol.

While selective relaying outperforms all-active relaying in the case of point-to-point cooperative FSO systems [11], limiting the transmission to selected transceivers in the considered multipoint-to-multipoint scenario will imply that the information signals will be available only at selected receivers. This alternative solution is therefore equivalent to Selective Combining (SC) that is known to be outperformed by MRC [25]. In fact, MRC is preferred over other combining schemes since it maximizes the received SNR [25].

B. Basic System Parameters

1) Input-Output Relation: The FSO system under consideration is based on Intensity Modulation and Direct Detection (IM/DD). Consider the communication over the n-th link $\text{TRx}_{\text{A},n}$-$\text{TRx}_{\text{B},n}$. The received electrical signal at $\text{TRx}_{\text{B},n}$ can be written as:

$$\mathfrak{r}_n = \eta h_n \mathfrak{s}_n + \mathfrak{w}_n, \tag{1}$$

where η is the optical-to-electrical conversion ratio and $\mathfrak{w}_n$ is the noise at transceiver $\text{TRx}_{\text{B},n}$ that is assumed to be additive white Gaussian noise (AWGN) with zero mean and variance $N_0/2$.

2) Channel Scintillation: In (1), h_n stands for the irradiance along the n-th link. The channel irradiances $\{h_n\}_{n=1}^N$ are assumed to be independent and identically distributed following from the facts that the distances of the links $\text{TRx}_{\text{A},n}$-$\text{TRx}_{\text{B},n}$ are approximately the same while the transceivers $\{\text{TRx}_{\text{A},n}\}_{n=1}^N$, on one hand, and $\{\text{TRx}_{\text{B},n}\}_{n=1}^N$, on the other hand, are sufficiently separated. The assumption of channel independence is valid since the separation between the multiuser transceivers deployed on a certain building easily exceeds the FSO channel coherence distance that is in the order of centimeters. In this work, we adopt a channel model that takes into account the combined effects of path loss, atmospheric turbulence-induced scintillation and misalignment-induced fading caused by pointing errors. Assuming a gamma-gamma turbulence model and a Gaussian spatial intensity profile falling on a circular aperture at the receiver, the probability density function (pdf) of the channel irradiance was derived in [26] and expressed in terms of the Meijer G-function $G_{p,q}^{m,n}[.]$ as follows:

$$f_{\gamma\gamma}(h) = \frac{\varphi_1\varphi_2\xi^2}{Ah^{(l)}\Gamma(\varphi_1)\Gamma(\varphi_2)} G_{1,3}^{3,0}\left[\frac{\varphi_1\varphi_2}{Ah^{(l)}}h\Big|_{\xi^2-1,\varphi_1-1,\varphi_2-1}^{\xi^2}\right], \tag{2}$$

where $\Gamma(.)$ is the Gamma function while φ_1 and φ_2 stand for the parameters of the distribution:

$$\varphi_1 = \left[\exp\left(0.49\sigma_R^2/(1+1.11\sigma_R^{12/5})^{7/6}\right) - 1\right]^{-1}, \tag{3}$$

$$\varphi_2 = \left[\exp\left(0.51\sigma_R^2/(1+0.69\sigma_R^{12/5})^{5/6}\right) - 1\right]^{-1}, \tag{4}$$

where $\sigma_R^2 = 1.23C_n^2k^{7/6}d^{11/6}$ is the Rytov variance, d is the link distance, $k = \frac{2\pi}{\lambda}$ is the wave number and C_n^2 denotes the refractive index structure parameter. In (2), the parameters A and ξ capture the effect of pointing errors. $A = \text{erf}^2(v)$ where erf(.) is the error function with $v = \sqrt{\pi/2}(a/\omega_z)$ where a is the radius of the receiver and ω_z is the beam waist. $\xi = \omega_{z_{eq}}/2\sigma_s$ where σ_s stands for the pointing error displacement standard deviation at the receiver and $\omega_{z_{eq}}^2 = \omega_z^2\sqrt{\pi}\text{erf}(v)/[2ve^{-v^2}]$. Finally, the atmospheric loss is given by $h^{(l)} = e^{-\sigma d}$ where σ is the attenuation coefficient [26]. It is worth noting that large values of ω_z and small values of σ_s will result in large values of ξ corresponding to the case of less severe pointing errors.

The cumulative distribution function (cdf) of the channel irradiance can be written as [26]:

$$F_{\gamma\gamma}(h) = \frac{\xi^2}{\Gamma(\varphi_1)\Gamma(\varphi_2)} G_{2,4}^{3,1}\left[\frac{\varphi_1\varphi_2}{Ah^{(l)}}h\Big|_{\xi^2,\varphi_1,\varphi_2,0}^{1,\xi^2+1}\right]. \tag{5}$$

[1]Note that information is often encrypted before transmission. Therefore, the availability of information to all users through the added wires will not affect the secrecy of the communications.

3) Modulation: In (1), the non-negative symbols $\mathfrak{s}_n$ that are suitable for IM/DD FSO systems are carved from the following M-ary Pulse Amplitude Modulation (PAM) constellation:

$$\mathcal{C}_M = \{m(2A)\ ,\ m = 0, \ldots, M-1\}, \tag{6}$$

of which the popular On-Off-Keying (OOK) constellation stands as a special case with $M = 2$. Normalizing the energy of the signal set in (6) can be realized by setting $A^2 = \frac{3}{2(M-1)(2M-1)}$.

4) Demodulation: For OOK that is deployed in the conventional scenario, a threshold is set at $\gamma_{th} = \eta A h_n$ and the Maximum-Likelihood (ML) decoder decides in favor of $\hat{m} = 0$ if $\mathfrak{r}_n \leq \gamma_{th}$ and $\hat{m} = 1$ otherwise. For the cooperative scheme with M-PAM, MRC is applied and the decision on the symbol transmitted by users in $\mathcal{S}_i$ will be based on the decision variable $\mathfrak{r} \triangleq \sum_{n\in\mathcal{S}_i} h_n \mathfrak{r}_n$. In this case, setting $\gamma_{th} = \eta A \sum_{n\in\mathcal{S}_i} h_n^2$, the receiver decides in favor of $\hat{m}$ if $\mathfrak{r} \in [L_{\hat{m}}\ U_{\hat{m}}]$ where $(L_0, U_0) = (-\infty, \gamma_{th})$, $(L_{M-1}, U_{M-1}) = ((2M-3)\gamma_{th}, +\infty)$ and $(L_m, U_m) = ((2m-1)\gamma_{th}, (2m+1)\gamma_{th})$ for $m \in \{1, \ldots, M-2\}$.

It is worth noting that while the information bits of the users in $\mathcal{S}_i$ are different, the same decision variable $\mathfrak{r}$ is used for the reconstruction of these bits. In fact, based on the proposed cooperation scheme, the users' bits are used to generate a single PAM symbol that is transmitted concurrently by all users in $\mathcal{S}_i$. Since the sequence of $|\mathcal{S}_i|$ bits can assume $2^{|\mathcal{S}_i|}$ possible values, then the PAM symbol needs to be carved from a $2^{|\mathcal{S}_i|}$-ary constellation where a one-to-one relation is applied between the bit sequences and the PAM symbols. In this context, the $|\mathcal{S}_i|$ replicas of the PAM symbol that are available at the receiver side need to be combined to generate $\mathfrak{r}$. Once $\mathfrak{r}$ has been calculated, the PAM symbol can be reconstructed based on the previously described decision rule. Now, the values of the $|\mathcal{S}_i|$ information bits can be deduced following from the one-to-one relation. Finally, the joint encoding corresponds to a simple mapping of the $|\mathcal{S}_i|$ users' bits to a $2^{|\mathcal{S}_i|}$-ary PAM symbol and can be carried out in a straightforward manner without incurring significant delays in the system. In all circumstances, this delay does not exceed a fraction of the symbol duration and is very small compared to the delays introduced by the scheduling schemes in [17]–[22] where a user can be deprived from accessing the channel for entire coherence blocks that extend over thousands of symbol durations.

5) Implementation and Complexity: The additional cost of the proposed solution arises from the additional cabling and the joint modulator/demodulator units. It can be observed that upgrading an existing FSO system to implement the proposed cooperation scheme incurs only marginal levels of additional complexity. In fact, even in the noncooperative case, all the channel iraddiances $h_1, \ldots, h_N$ need to be estimated where each irradiance is estimated by the corresponding user for the sake of fixing the threshold of the ML detector. In this context, the proposed cooperation scheme does not require the estimation of any additional parameters. On the other hand, the transmission of the jointly encoded symbols does not induce any bandwidth expansion since all M-PAM constellations occupy the same bandwidth. Moreover, the data rate of each user is kept the same. Finally, synchronizing the communication between buildings (A) and (B) is simple and comparable to the noncooperative case since all users transmit in a concurrent manner while the distances between any pair of transceivers are roughly the same. In all circumstances, this synchronization is by far less challenging compared to relay-assisted networks.

III. Performance Analysis: Preliminaries and Special Cases

A. Approximate pdf's and cdf's

The pdf in (2) does not lend itself to simple closed-form evaluation. Therefore, for the sake of deriving closed-from expressions of the asymptotic error probability, we resort to approximating this pdf by the following expression near the origin [27]:

$$f_{\gamma\gamma}(h) \approx a h^{\beta-1} \triangleq \frac{\xi^2(\varphi_1\varphi_2)^\beta \Gamma(\varphi_1-\beta) b}{(A h^{(l)})^\beta \Gamma(\varphi_1)\Gamma(\varphi_2)} h^{\min\{\varphi_2, \xi^2\}-1}. \tag{7}$$

where $b = 1/(\xi^2 - \varphi_2)$ if $\xi^2 > \varphi_2$ and $b = \Gamma(\varphi_2 - \xi^2)$ if $\xi^2 < \varphi_2$.

Based on this expression, the cdf in (5) can be approximated by:

$$F_{\gamma\gamma}(h) \approx \frac{a}{\beta} h^\beta = \frac{\xi^2(\varphi_1\varphi_2)^\beta \Gamma(\varphi_1-\beta) b}{(A h^{(l)})^\beta \Gamma(\varphi_1)\Gamma(\varphi_2)\beta} h^{\min\{\varphi_2, \xi^2\}}. \tag{8}$$

The performance evaluation with MRC necessitates the analysis of the random variable (r.v.) h^2. The cdf of this r.v. is obtained from: $F_{h^2}(x) = \Pr(h^2 \leq x) = \Pr(h \leq \sqrt{x}) = F_{\gamma\gamma}(\sqrt{x})$ where the second equality follows since the channel irradiance is positive. Consequently, from (8):

$$F_{h^2}(h) \approx \frac{a}{\beta} h^{\frac{\beta}{2}} = \frac{\xi^2(\varphi_1\varphi_2)^\beta \Gamma(\varphi_1-\beta) b}{(A h^{(l)})^\beta \Gamma(\varphi_1)\Gamma(\varphi_2)\beta} h^{\frac{\min\{\varphi_2, \xi^2\}}{2}}. \tag{9}$$

Differentiating (9) results in:

$$f_{h^2}(h) \approx \frac{a}{2} h^{\frac{\beta}{2}-1} \frac{\xi^2(\varphi_1\varphi_2)^\beta \Gamma(\varphi_1-\beta) b}{2(A h^{(l)})^\beta \Gamma(\varphi_1)\Gamma(\varphi_2)} h^{\frac{\min\{\varphi_2, \xi^2\}}{2}-1}. \tag{10}$$

B. BER Expressions

For the transmissions from the users in the set $\mathcal{S}$, the conditional Bit Error Rate (BER) with unipolar M-PAM and MRC can be written as ($M = 2^{|\mathcal{S}|}$):

$$P_{e|H}(\mathcal{S}) = \frac{2(M-1)}{M\log_2 M} Q\left(\sqrt{\frac{3\log_2 M}{(M-1)(2M-1)} \frac{\eta^2 E_b}{N_0} \sum_{n\in\mathcal{S}} h_n^2}\right), \tag{11}$$

where the relation $M = 2^{|\mathcal{S}|}$ follows since the generated symbol encompasses the $|\mathcal{S}|$ information bits of the involved user. In (11), E_b stands for the energy of an information bit while $Q(x) = \frac{1}{\sqrt{2\pi}} \int_x^\infty e^{-\frac{t^2}{2}} \mathrm{d}t$ is the Q-function.

Averaging (11) over the channel irradiances results in the following expression of the BER:

$$P_e(\mathcal{S}) = \frac{2(M-1)}{M\log_2 M} \int_0^{+\infty} Q\left(\sqrt{\frac{3\log_2 M}{(M-1)(2M-1)} \frac{\eta^2 E_b}{N_0} h}\right) \times f_{\sum_{n\in\mathcal{S}} h_n^2}(h)\mathrm{d}h \ \ ; \ \ M = 2^{|\mathcal{S}|}, \tag{12}$$

where $f_{\sum_{n\in\mathcal{S}} h_n^2}(h)$ stands for the pdf of the r.v. $\sum_{n\in\mathcal{S}} h_n^2$.

C. Diversity Order

A useful metric for capturing the performance of diversity systems is the diversity order defined as the negative slope of the BER curve on a log-log plot for large values of the SNR: $\delta = -\lim_{\frac{E_b}{N_0}\to+\infty} \frac{\partial \log(P_e(\mathcal{S}))}{\partial \log\left(\frac{E_b}{N_0}\right)}$.

In an attempt to evaluate the achievable diversity orders, we observe that the tails of the pdf's of the different involved r.v.s can be written under the following general form:

$$f_{\sum_{n\in\mathcal{S}} h_n^2}(h) \approx \mu_{\mathcal{S}} h^{\nu_{\mathcal{S}}-1}, \tag{13}$$

where $\mu_{\mathcal{S}}$ and $\nu_{\mathcal{S}}$ are two constants that depend on the set $\mathcal{S}$ and on the channel parameters. The form in (13) follows from applying the Taylor series expansion and constitutes a valid approximation near the origin that is useful in deriving the asymptotic BERs. Replacing (13) in (12) while approximating $Q(x)$ by $\frac{1}{\sqrt{2\pi}x}e^{-\frac{x^2}{2}}$ results in the following expression of the BER:

$$P_e(\mathcal{S}) = \frac{\mu_{\mathcal{S}}}{2\sqrt{\pi}} \frac{2(M-1)}{M\log_2 M}\Gamma\left(\nu_{\mathcal{S}}-\frac{1}{2}\right)\times \left(\frac{3\log_2 M}{(M-1)(2M-1)}\frac{\eta^2 E_b}{2N_0}\right)^{-\nu_{\mathcal{S}}} \quad ; \quad M=2^{|\mathcal{S}|}, \tag{14}$$

showing that the achievable diversity order is equal to $\nu_{\mathcal{S}}$.

It is worth noting that the approximations of the irradiance-pdf and the Q-function are both coherent with the asymptotic analysis that we develop throughout this paper. In fact, $Q(x)$ approaches the approximate value of $\frac{1}{\sqrt{2\pi}x}e^{-\frac{x^2}{2}}$ for $x \geq 3$ where this condition is easily satisfied for asymptotically large values of the SNR. In other words, consider the term $\frac{E_b}{N_0}h$ that appears inside the Q-function in (12). At asymptotic SNRs ($\frac{E_b}{N_0} \to \infty$), this term will be very large for average-to-large values of the channel irradiance h resulting in small values of the Q-function and, hence, in minor contribution of the corresponding terms to the BER. This justifies the predominant effect that small values of h have on the asymptotic BER justifying performing the Taylor series expansion of the pdf near the origin. Note that for exceedingly small values of h, the argument of the Q-function in (12) might be smaller than 3 highlighting a slight discrepancy between the exact and approximate expressions. This discrepancy is small since there is a small probability of h assuming such extremely small values since the pdf in (2) is zero at the origin. In all circumstances, the function $\frac{1}{\sqrt{2\pi}x}e^{-\frac{x^2}{2}}$ serves as an upper-bound of $Q(x)$ for $x \geq 0$.

D. Noncooperative Scenario

For the noncooperative scheme, the conditional BER can be obtained from (11) as follows:

$$P_{e|H}^{(0)} = \left.\frac{2(M-1)}{M\log_2 M} Q\left(\sqrt{\frac{3\log_2 M}{(M-1)(2M-1)}\frac{\eta^2 E_b}{N_0}h^2}\right)\right]_{M=2} = Q\left(\sqrt{\frac{\eta^2 E_b}{N_0}h^2}\right), \tag{15}$$

where the pdf of the r.v. h is given in (2).

Following from (10), the pdf of h^2 can be written under the form given in (13) with $\mu_{\mathcal{S}} = \frac{a}{2}$ and $\nu_{\mathcal{S}} = \frac{\beta}{2}$. Replacing these values (along with $M = 2$) in (14) results in:

$$P_e^{(0)} \approx \frac{a}{4\sqrt{\pi}}\Gamma\left(\frac{\beta-1}{2}\right)\left(\frac{\eta^2 E_b}{2N_0}\right)^{-\frac{\beta}{2}}, \tag{16}$$

where in (15) and (16) the superscript 0 is used to denote the conventional noncooperative scheme. $P_{e|H}^{(0)}$ stands for the error probability that is conditioned on the channel state set $H = \{h_1, \ldots, h_N\}$ that reduces to the single channel irradiance in the single-user scenario. Similarly, the average error probability $P_e^{(0)}$ is obtained by integrating $P_{e|H}^{(0)}$ over the pdf of the channel irradiance. Equation (16) shows that the diversity order in the noncooperative scenario is equal to $\beta/2$ in coherence with the previously reported results in the open literature on FSO.

E. All-User Grouping

A special case of the proposed cooperation scheme corresponds to all-user grouping. In this case, a 2^N-ary PAM symbol is generated comprising the information from all N users. This symbol is then transmitted by the transceivers of all users along the N available optical links. In other words, the set $\{1, \ldots, N\}$ is not partitioned and the symbols are carved from a 2^N-ary PAM constellation. From (11), this results in the following expression of the conditional BER:

$$P_{e|H}(\{1,\ldots,N\}) = \frac{2^N-1}{N2^{N-1}}\times Q\left(\sqrt{\frac{3N}{(2^N-1)(2^{N+1}-1)}\frac{\eta^2 E_b}{N_0}\sum_{n=1}^{N} h_n^2}\right). \tag{17}$$

The r.v. $\sum_{n=1}^{N} h_n^2$ corresponds to the summation of N independent and identically-distributed random variables. Following from the approximation in (10), the corresponding pdf can be written as: $f_{\sum_{n=1}^{N} h_n^2}(h) = \left(\frac{a}{2}\right)^N \left[h^{\frac{\beta}{2}-1} * \cdots * h^{\frac{\beta}{2}-1}\right]$ where the convolution $*$ needs to be performed $N-1$ times. Applying the same calculation steps as in [28] results in:

$$f_{\sum_{n=1}^{N} h_n^2}(h) = \left(\frac{a}{2}\right)^N \frac{\Gamma^N(\beta/2)}{\Gamma(N\beta/2)} h^{\frac{N\beta}{2}-1}, \tag{18}$$

showing that this pdf can be written under the form in (13) with $\mu_{\{1,\ldots,N\}} = \left(\frac{a}{2}\right)^N \frac{\Gamma^N(\beta/2)}{\Gamma(N\beta/2)}$ and $\nu_{\{1,\ldots,N\}} = \frac{N\beta}{2}$. Replacing these values (as well as $M = 2^N$) in (14) results in:

$$P_e(\{1,\ldots,N\}) \approx \frac{a^N}{\sqrt{\pi}}\frac{2^N-1}{N2^{2N}}\frac{\Gamma^N\left(\frac{\beta}{2}\right)\Gamma\left(\frac{N\beta-1}{2}\right)}{\Gamma\left(\frac{N\beta}{2}\right)}\times \left(\frac{3N}{(2^N-1)(2^{N+1}-1)}\right)^{-\frac{N\beta}{2}}\left(\frac{\eta^2 E_b}{2N_0}\right)^{-\frac{N\beta}{2}}. \tag{19}$$

Equation (19) shows that the BER scales asymptotically as $\left(\frac{E_b}{N_0}\right)^{-\frac{N\beta}{2}}$ revealing an N-fold increase in the achievable diversity order. However, our subsequent analysis will show

that the multiplicative term in (19) increases very rapidly with N showing that the increase in the diversity order might be jeopardized by the performance losses induced by the expansion of the initial OOK constellation especially at low-to-average SNRs.

Finally, it is worth noting that while the parameters $(\mu_{\mathcal{S}}, \nu_{\mathcal{S}})$ assume the values of $\left(\frac{a}{2}, \frac{\beta}{2}\right)$ and $\left(\frac{a^N \Gamma^N(\beta/2)}{2^N \Gamma(N\beta/2)}, \frac{N\beta}{2}\right)$ in the noncooperative and all-user-grouping scenarios, respectively, their expressions are much more challenging to derive for an arbitrary cooperating group $\mathcal{S}$ as will be highlighted in the subsequent section.

IV. Performance Analysis with N Users

A. Channel Ordering and User Grouping

The partitioning of the N users into different groups will be based on the values of the channel irradiances. For simplicity of notation, we assume that the channel irradiances are arranged in an increasing order:

$$h_1 \leq h_2 \leq \cdots \leq h_N, \tag{20}$$

where it is worth noting that this sorting does not affect the analysis presented in Subsection III-E since the sets of all sorted and unsorted irradiances are the same.

Consequently, in the subsequent analysis, the channel irradiances will be perceived as sample order statistics with h_1 corresponding to the *worst* FSO link, h_2 to the second *worst* link, ... and h_N to the *best* link. In this context, even though the FSO channels are independent and identically distributed, the newly generated order statistics $h_1, \ldots, h_N$ are neither independent nor identically distributed because of the order restriction. For example, with $N = 5$, the partitioning $\{\{1, 2, 3\}, \{4, 5\}\}$ means that 4-PAM symbols are transmitted over the two strongest channels while 8-PAM symbols are transmitted over the three weakest channels.

B. Classes of Service

Evidently, any grouping other than the all-user grouping will be capable of providing different classes of service to the different users in the network. The users can be classified as gold users, silver users, bronze users... where the corresponding BERs are arranged in an increasing order. In this context, we denote the BER of the n-th best user by $P_e^{(n)}$ for $n = 1, \ldots, N$ with $P_e^{(1)} \leq \cdots \leq P_e^{(N)}$. For practical implementation of the proposed collaborative scheme, the entities that have invested the most for covering the additional cost incurred by the upgrade of the system (cabling, hardware...) can be selected as the gold users who will profit from the highest Quality-of-Service (QoS). Other entities that are not willing to embrace additional costs can be designated as the silver or bronze users who can still profit from enhanced QoS just by making their transceivers accessible for cooperation. This gives an incentive for all users to participate in the cooperation effort since their QoSs will be enhanced compared to noncooperative networks. In all circumstances, users that are not willing to cooperate, for one reason or another, are to be excluded from the set $\{1, \ldots, N\}$. In this context, N corresponds to the number of users that are willing to cooperate (rather than the total number of existing users) and cooperation is limited to these users in a way that is completely analogous to the point-to-point cooperative systems.

The average BER of the N-user system under user cooperation can be evaluated from:

$$P_{sys} = \frac{1}{N} \sum_{n=1}^{N} P_e^{(n)}. \tag{21}$$

Evidently, the BER of the system will be dominated by that of the worst user and the corresponding achievable diversity order would be:

$$\delta_{sys} = \min_{n=1,\ldots,N} \delta^{(n)}, \tag{22}$$

where $\delta^{(n)}$ is the diversity order of the n-th best user.

Finally, the partitioning $\{1, \ldots, N\} = \{1\} \cup \cdots \cup \{N\}$ corresponds to a simple reordering of the users and it is equivalent to the noncooperative scenario.

C. PDF of the r.v. $\sum_{n\in\mathcal{S}} h_n^2$ near the origin

A key point in our analysis corresponds to writing the pdf of the r.v. $\sum_{n\in\mathcal{S}} h_n^2$ under the form given in (13) in an attempt to derive the diversity order resulting from the joint transmission of the users in $\mathcal{S}$. Before tackling the general case of sets with an arbitrary number of elements, we first consider the special cases of sets with one, two and three users. This approach is useful in offering more insights on the derivation steps and in introducing the different involved variables.

1) Special Case: $|\mathcal{S}| \leq 3$:

Proposition 1: [$|\mathcal{S}| = 1$]: For any value of N, the pdf of the r.v. h_i^2 corresponding to the i-th best channel can be approximated by the following expression near the origin:

$$f_{h_i^2}(h) \approx \frac{N!}{2(i-1)!(N-i)!} a^i \beta^{1-i} h^{i\frac{\beta}{2}-1} \triangleq \mu_{\{i\}} h^{\nu_{\{i\}}-1}. \tag{23}$$

Proof: Based on order statistics, the pdf of h_i^2 is given by [29, 2.2.2]:

$$f_{h_i^2}(h) = \frac{N!}{(i-1)!(N-i)!} f_{h^2}(h) \left[F_{h^2}(h)\right]^{i-1} \left[1 - F_{h^2}(h)\right]^{N-i}. \tag{24}$$

Replacing the pdf and cdf of h^2 by the approximate expressions given in (9)-(10) and ignoring the high order terms near the origin results in the expression given in (23). ■

Proposition 2: [$|\mathcal{S}| = 2$]: For any value of N, the pdf of the r.v. $h_i^2 + h_j^2$ with $1 \leq i < j \leq N$ (resulting in $h_i < h_j$ and $h_i^2 < h_j^2$) can be approximated by the following expression:

$$f_{h_i^2+h_j^2}(h) \approx \left[\frac{N!}{4(i-1)!(j-i-1)!(N-j)!} a^j \beta^{2-j} (-1)^{j-i-1} \times \sum_{m=0}^{j-i-1} \binom{j-i-1}{m} (-1)^m B\left(\frac{1}{2}; \frac{\beta}{2}(j-m-1), \frac{\beta}{2}(m+1)\right)\right] h^{j\frac{\beta}{2}-1}$$
$$\triangleq \mu_{\{i,j\}} h^{\nu_{\{i,j\}}-1}, \tag{25}$$

where $B(z; a, b)$ stands for the incomplete beta function: $B(z; a, b) = \int_0^z u^{a-1}(1-u)^{b-1} \mathrm{d}u$ [30].

Proof: The proof is provided in Appendix A. ■

$$\mu_{\{i,j,k\}} = \frac{N!}{8(i-1)!(j-i-1)!(k-j-1)!(N-k)!} a^k \beta^{3-k} (-1)^{k-i} \sum_{m=0}^{j-i-1} \binom{j-i-1}{m} (-1)^m \sum_{m'=0}^{k-j-1} \binom{k-j-1}{m'} (-1)^{m'} \left[B\left(\frac{1}{2}; (k-j+m-m')\frac{\beta}{2}, (m'+1)\frac{\beta}{2}\right) B\left(\frac{1}{3}; (j-m-1)\frac{\beta}{2}, (k-j+m+1)\frac{\beta}{2}\right) - \sum_{r=0}^{+\infty} \frac{\left(1-(m'+1)\frac{\beta}{2}\right)_r}{\left((k-j+m-m')\frac{\beta}{2}+r\right) r!} B\left(\frac{1}{3}; (k-m'-1)\frac{\beta}{2}+r, (m'+1)\frac{\beta}{2}-r\right) \right], \quad (27)$$

Proposition 3: [$|\mathcal{S}| = 3$]: For any value of N, the pdf of the r.v. $h_i^2 + h_j^2 + h_k^2$ with $1 \leq i < j < k \leq N$ can be approximated by the following expression near the origin:

$$f_{h_i^2+h_j^2+h_k^2}(h) \approx \mu_{\{i,j,k\}} h^{k\frac{\beta}{2}-1} \triangleq \mu_{\{i,j,k\}} h^{\nu_{\{i,j,k\}}-1}, \quad (26)$$

where $\mu_{\{i,j,k\}}$ is given in (27) at the top of the page where $(x)_n$ stands for the Pochhammer symbol: $(x)_n \triangleq \frac{\Gamma(x+n)}{\Gamma(x)}$.

Proof: The proof is provided in Appendix B. ■

Corollary 1: The transmissions over the i-th, (i,j)-th and (i,j,k)-th best channels (with $i < j < k$) result in i-fold, j-fold and k-fold increases in the diversity order, respectively.

Proof: The proof follows directly from (14) since the pdf's in (23), (25) and (26) can be written under the general form provided in (13) with $\nu_{\mathcal{S}}$ being equal to $\nu_{\{i\}} = i\frac{\beta}{2}$, $\nu_{\{i,j\}} = j\frac{\beta}{2}$ and $\nu_{\{i,j,k\}} = k\frac{\beta}{2}$, respectively. ■

2) General Case: Consider now the general case $|\mathcal{S}| = N_{\mathcal{S}}$ where the set $\mathcal{S}$ is written as $\mathcal{S} = \{i_1, \ldots, i_{N_{\mathcal{S}}}\}$ with $i_1 < \cdots < i_{N_{\mathcal{S}}}$.

Proposition 4: For any value of N, the pdf of the r.v. $h_{i_1}^2 + \cdots + h_{i_{N_{\mathcal{S}}}}^2$ with $1 \leq i_1 < \cdots < i_{N_{\mathcal{S}}} \leq N$ can be approximated by the following expression near the origin:

$$f_{\sum_{n\in\mathcal{S}} h_n^2}(h) \approx \mu_{\mathcal{S}} h^{\max\{\mathcal{S}\}\frac{\beta}{2}-1}, \quad (28)$$

where $\mu_{\mathcal{S}}$ is given in (29) at the top of the next page.

In (29), the constants $\{P_n\}_{n=1}^{N_{\mathcal{S}}}$ are given by:

$$P_n = \begin{cases} \frac{\beta}{2}(i_2 - 1 - m_1), & n = 1; \\ \frac{\beta}{2}(i_{n+1} - i_n + m_{n-1} - m_n), & n = 2, \ldots, N_{\mathcal{S}} - 1; \\ \frac{\beta}{2}(1 + m_{N_{\mathcal{S}}-1}), & n = N_{\mathcal{S}}. \end{cases} \quad (30)$$

while the constants $\{\xi_{r_n}\}_{n=1}^{N_{\mathcal{S}}-2}$ are determined sequentially according to the following relation if $r_n < 0$:

$$\xi_{r_n} = B\left(\frac{1}{n+1}; \sum_{n'=1}^{n} P_{N_{\mathcal{S}}-n'} + \sum_{n'=1}^{n-1} r_{n'}, P_{N_{\mathcal{S}}} - \sum_{n'=1}^{n-1} r_{n'}\right), \quad (31)$$

and according to the following relation if $r_n \geq 0$:

$$\xi_{r_n} = -\frac{\left(1 - P_{N_{\mathcal{S}}} + \sum_{n'=1}^{n-1} r_{n'}\right)_{r_n}}{\left(\sum_{n'=1}^{n} P_{N_{\mathcal{S}}-n'} + \sum_{n'=1}^{n} r_{n'}\right) r_n!}. \quad (32)$$

Finally, the sets $\mathcal{R}_1, \ldots, \mathcal{R}_{N_{\mathcal{S}}-2}$ are given by:

$$\mathcal{R}_n = \left\{ -\sum_{n'=1}^{n} P_{N_{\mathcal{S}}-n'} - \sum_{n'=1}^{n-1} r_{n'} \right\} \cup \mathbb{N} \; ; \; n = 1, \ldots, N_{\mathcal{S}} - 2, \quad (33)$$

where $\mathbb{N}$ stands for the set of natural integers. In this case, each one of these sets comprises one negative integer and an infinite number of positive integers.

Proof: The proof is provided in Appendix C. ■

A simple replacement of the involved variables by their corresponding values shows that (29) simplifies to the expressions provided in (25) and (26)-(27) for $N_{\mathcal{S}} = 2$ and $N_{\mathcal{S}} = 3$, respectively.

Corollary 2: The joint transmission over the channels $\{h_n\}_{n\in\mathcal{S}}$ allows to increase the diversity order by a factor that is equal to $\max\{\mathcal{S}\}$.

Proof: The proof follows directly from (14) since the pdf in (29) can be written under the general form provided in (13) with $\nu_{\mathcal{S}} = i_{N_{\mathcal{S}}}\frac{\beta}{2} = \max\{\mathcal{S}\}\frac{\beta}{2}$. ■

Several conclusions pertaining to the partitioning of the users can be drawn from corollary 2. For instance, if $\{1, \ldots, N\}$ is partitioned into L subsets $\mathcal{S}_1 \cup \cdots \cup \mathcal{S}_L$, then the diversity order of the system can be expressed as $\delta_{sys} = \frac{\beta}{2}\min\{\max\{\mathcal{S}_1\}, \ldots, \max\{\mathcal{S}_L\}\}$ following from (22). Therefore, the values $N, N-1, \ldots, N-(L-1)$ must be each included in one of the subsets $\mathcal{S}_1, \ldots, \mathcal{S}_L$ in order to result in an advantage in the achievable user diversity orders for the same modulation orders. In this case, for a fixed value of L, the system diversity order will be $\delta_{sys} = [N-(L-1)]\frac{\beta}{2}$. All of these findings allow to disregard numerous groupings of the set $\{1, \ldots, N\}$. For example, the partitioning $\{\{1,2,3\},\{4,5,6\}\}$ must be excluded from the candidate groupings since the alternative option $\{\{1,2,5\},\{3,4,6\}\}$ allows to achieve a higher diversity order while transmitting the same modulated signal sets (two 8-ary constellations).

D. Extension of the Results to EGC

In what follows, we extend the obtained results to the case of Equal-Gain Combining (EGC) that constitutes a simple alternative to MRC. When EGC is applied, the conditional BER in (11) takes the following expression: $P_{e|H}(\mathcal{S}) = \frac{2(M-1)}{M\log_2 M} Q\left(\sqrt{\frac{3\log_2 M}{(M-1)(2M-1)}\frac{\eta^2 E_b}{NN_0}\left(\sum_{n\in\mathcal{S}} h_n\right)^2}\right)$. In a way similar to (13), the pdf of the r.v. $\left(\sum_{n\in\mathcal{S}} h_n\right)^2$ can be written under the form:

$$f_{\left(\sum_{n\in\mathcal{S}} h_n\right)^2}(h) \approx \mu'_{\mathcal{S}} h^{\nu'_{\mathcal{S}}-1}, \quad (34)$$

where, in what follows, $(\mu'_{\mathcal{S}}, \nu'_{\mathcal{S}})$ (for EGC) will be related to $(\mu_{\mathcal{S}}, \nu_{\mathcal{S}})$ (for MRC).

Equation (34) implies that $f_{\sum_{n\in\mathcal{S}} h_n}(h) = 2\mu'_{\mathcal{S}} h^{2\nu'_{\mathcal{S}}-1}$ which will be compared with $f_{\sum_{n\in\mathcal{S}} h_n^2}(h) = \mu_{\mathcal{S}} h^{\nu_{\mathcal{S}}-1}$ from (13). Equations (7)-(10) show that the pdf and cdf of h_n can be

$$\mu_{\mathcal{S}} = \Bigg[\frac{N!}{2^{N_{\mathcal{S}}}(i_1-1)!(N-i_{N_{\mathcal{S}}})!} a^{i_{N_{\mathcal{S}}}} \beta^{N_{\mathcal{S}}-i_{N_{\mathcal{S}}}} \sum_{m_1=0}^{i_2-i_1-1} \cdots \sum_{m_{N_{\mathcal{S}}-1}=0}^{i_{N_{\mathcal{S}}}-i_{N_{\mathcal{S}}-1}-1} (-1)^{i_{N_{\mathcal{S}}}-i_1-(N_{\mathcal{S}}-1)-\sum_{j=1}^{N_{\mathcal{S}}-1} m_j}$$
$$\prod_{j=1}^{N_{\mathcal{S}}-1} \frac{\binom{i_{j+1}-i_j-1}{m_j}}{(i_{j+1}-i_j-1)!} \sum_{r_1 \in \mathcal{R}_1} \cdots \sum_{r_{N_{\mathcal{S}}-2} \in \mathcal{R}_{N_{\mathcal{S}}-2}} \xi_{r_1} \cdots \xi_{r_{N_{\mathcal{S}}-2}} B\left(\frac{1}{N_{\mathcal{S}}}; \sum_{n'=1}^{N_{\mathcal{S}}-1} P_{N_{\mathcal{S}}-n'} + \sum_{n'=1}^{N_{\mathcal{S}}-2} r_{n'}, P_{N_{\mathcal{S}}} - \sum_{n'=1}^{N_{\mathcal{S}}-2} r_{n'}\right) \Bigg] h^{i_{N_{\mathcal{S}}}\frac{\beta}{2}-1}. \quad (29)$$

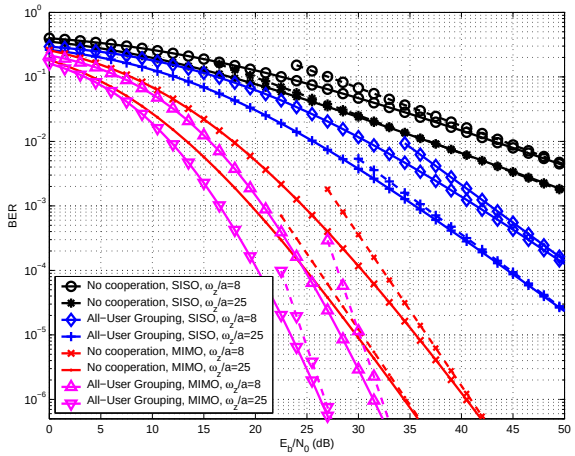

Fig. 2. Performance with $N = 2$ users. Solid and dashed lines correspond to the exact and approximate BERs, respectively.

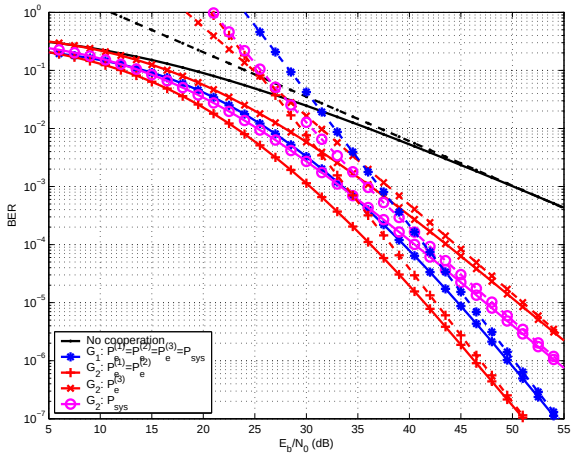

Fig. 3. Performance with $N = 3$ users. Solid and dashed lines correspond to the exact and approximate BERs, respectively.

obtained from the pdf and cdf of h_n^2, respectively, by replacing a with $2a$ and β with 2β. Therefore, the BER expressions with EGC can be obtained from the BER expressions with MRC by (i): dividing the SNR by N and (ii): replacing $\mu_{\mathcal{S}}$ with $\mu'_{\mathcal{S}}$ and $\nu_{\mathcal{S}}$ with $\nu'_{\mathcal{S}}$ in all of the previously derived approximate expressions. In this case, $\mu'_{\mathcal{S}}$ (resp. $\nu'_{\mathcal{S}}$) can be obtained from $\mu_{\mathcal{S}}$ (resp. $\nu_{\mathcal{S}}$) by replacing a with $2a$, β with 2β while dividing the obtained answer by 2. Performing this operation with $\nu_{\mathcal{S}} = \max\{\mathcal{S}\}\frac{\beta}{2}$, from (29), results in $\nu'_{\mathcal{S}} = \frac{1}{2}\max\{\mathcal{S}\}\frac{2\beta}{2} = \nu_{\mathcal{S}}$ showing that MRC and EGC are capable of achieving the same diversity order.

V. Candidate Groupings and Numerical Analysis

In this section, we compare the candidate user groupings over atmospheric turbulent channels that suffer from scintillation and pointing errors. The refractive index structure constant and the attenuation constant are set to $C_n^2 = 1{\times}10^{-14}$ $\mathrm{m}^{-2/3}$ and $\sigma = 0.44$ dB/km, respectively. The optical-to-electrical conversion ratio and the operating wavelength are set to the $\eta = 0.5$ and $\lambda = 1550$ nm, respectively. In what follows, we set $\sigma_s/a = 3$ while the values of ω_z/a will be varied in the simulations where large values of this ratio indicate less pointing errors. In this section, the exact BERs are obtained by numerically averaging the conditional BERs over the corresponding pdf's that, in their turn, were evaluated numerically. This numerical method is applied since the exact pdf's (of the sum of n sorted channel irradiances) can not be evaluated analytically. An extensive simulation campaign highlighted the extremely close match between the numerical results and Monte Carlo simulations.

A. Cooperation with $N = 2$ Users

The only grouping option with two users corresponds to the all-user grouping analyzed in Subsection III-E. In this case, $P_{sys} = P_e^{(1)} = P_e^{(2)}$ where the conditional and asymptotic BERs can be obtained by replacing $N = 2$ in (17) and (19), respectively. This grouping results in a two-fold increase in the diversity order from $\beta/2$ to β.

Fig. 2 shows the performance over a 5 km link for $\omega_z/a = 8$ and $\omega_z/a = 25$. For this simulation setup, $\varphi_1 = 4.92$ and $\varphi_2 = 1.17$ while $\xi = 1.34$ for $\omega_z/a = 8$ and $\xi = 4.17$ for $\omega_z/a = 25$. We also consider the cases of SISO and 2×2 MIMO transceivers. In the latter case, the transceivers of each one of the two users are equipped with two transmitting/receiving apertures. Results highlight the improved performance levels and diversity orders that are achieved by the proposed scheme under different pointing error conditions. Results also reflect the accuracy of the derived asymptotic BER expressions in approximating the performance for large values of the SNR. In this context, the approximate BERs are very close to the exact BERs for large SNRs and are hence useful in predicting the diversity order. In the case of two users, the cooperative scheme outperforms the noncooperative scheme for practically all values of the SNR and, consequently, the extension of the binary constellation to the 4-ary constellation was not very penalizing in this case. The performance gains are also evident in the case of MIMO transceivers. In this context, the proposed cooperative scheme constitutes a complement to MIMO solutions where the multiuser diversity achieved by the proposed scheme adds up to the spatial diversity achieved by deploying multiple apertures.

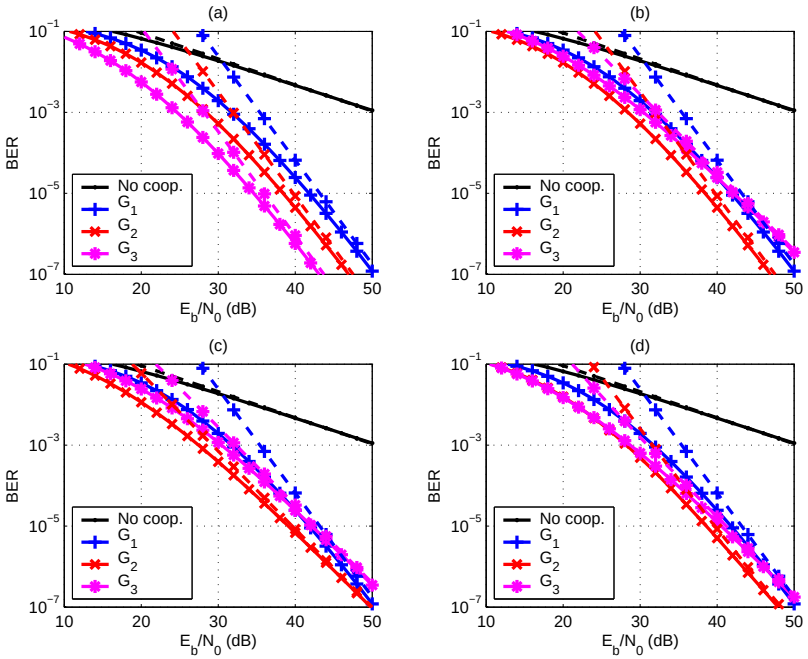

Fig. 4. Performance with $N = 4$ users. Solid and dashed lines correspond to the exact and approximate BERs, respectively. (a): $P_e^{(1)} = P_e^{(2)}$, (b): $P_e^{(3)}$, (c): $P_e^{(4)}$, (d): P_{sys}.

B. Cooperation with $N = 3$ Users

The possible groupings of the $N = 3$ users are as follows: $\{\{1,2,3\}\}$, $\{\{1\},\{2,3\}\}$, $\{\{2\},\{1,3\}\}$ and $\{\{3\},\{1,2\}\}$. Based on corollary 1 and following from (22), the groupings $\{\{1\},\{2,3\}\}$, $\{\{2\},\{1,3\}\}$ and $\{\{3\},\{1,2\}\}$ result in the diversity orders $\delta_{sys} = \min\{1, \max\{2,3\}\}\frac{\beta}{2} = \frac{\beta}{2}$, $\delta_{sys} = \min\{2, \max\{1,3\}\}\frac{\beta}{2} = \beta$ and $\delta_{sys} = \min\{3, \max\{1,2\}\}\frac{\beta}{2} = \beta$ implying that the first option must be disregarded. Regarding the remaining options $\{\{2\},\{1,3\}\}$ and $\{\{3\},\{1,2\}\}$ that both double the system diversity order, the first one is preferred for the following reasons. (i): In the first case, one user profits from the diversity order β and two users profit from the diversity order $3\frac{\beta}{2}$ while in the second case one user profits from the diversity order $3\frac{\beta}{2}$ and two users profit from the diversity order β. (ii): While in the first case the sole user with the smallest diversity order is transmitting 2-PAM symbols, the two users with the smallest diversity order are transmitting 4-PAM symbols in the second case. Keeping in mind that 4-PAM performs worse than 2-PAM, the first option is preferable since P_{sys} is dominated by the worst user.

As a conclusion, the candidate grouping options to be considered are $\{\{1,2,3\}\}$ and $\{\{2\},\{1,3\}\}$. In the second case, the weakest channel is *combined* with the strongest channel where these channels will carry the same 4-PAM symbol while the average channel carries regular 2-PAM symbols in order to avoid 8-ary modulation as in the first partitioning. The grouping $\{\{1,2,3\}\}$ is called G_1 for which $P_e^{(1)} = P_e^{(2)} = P_e^{(3)} = P_e(\{1,2,3\})$ whose asymptotic expression is given in (19). The grouping $\{\{2\},\{1,3\}\}$ is called G_2 for which $P_e^{(1)} = P_e^{(2)} < P_e^{(3)}$ resulting in a QoS differentiation between two gold users and one silver user. The asymptotic expression of $P_e^{(1)} = P_e^{(2)} = P_e(\{1,3\})$ is given in (14) with $\nu_{\{1,3\}} = 3\frac{\beta}{2}$ and $\mu_{\{1,3\}}$ as given in (25) while $P_e^{(3)} = P_e(\{2\})$ assumes the asymptotic value in (14) with $\nu_{\{2\}} = \beta$ and $\mu_{\{2\}}$ as given in (23).

The above grouping strategies are compared in Fig. 3 for a 3 km link and $\omega_z/a = 10$ ($\varphi_1 = 4.04$, $\varphi_2 = 1.53$ and $\xi = 1.67$). Results reflect the high performance gains that can be achieved by the proposed multiuser cooperation scheme. For G_1, the performance of each one of the users is enhanced by 16.5 dB at a BER of 10^{-3}; for G_2, the performance of the two gold users is enhanced by 19.5 dB while the performance of the third silver user is enhanced by around 13.75 dB at 10^{-3}. Regarding the average BER of the network, G_1 is evidently superior to G_2 for large SNRs which is expected since $\delta_{sys} = 3\frac{\beta}{2}$ for G_1 while $\delta_{sys} = \beta$ for G_2. However, for SNRs below 33 dB, G_2 manifests a slightly superior performance by about 0.5 dB.

C. Cooperation with $N = 4$ Users

Based on corollary 1 and the analysis presented in Subsection III-E, the best candidate grouping solutions in the case of $N = 4$ users are as follows:

- The all-user grouping $G_1 = \{\{1,2,3,4\}\}$ for which $\delta_{sys} = 2\beta$ where each one of the 4 users profits from the diversity order 2β while transmitting 16-PAM symbols.
- Grouping $G_2 = \{\{3\},\{1,2,4\}\}$ for which $\delta_{sys} = 3\frac{\beta}{2}$. For this grouping, 3 gold users profit from the diversity order 2β while transmitting 8-PAM symbols whereas the remaining user profits from the diversity order $3\frac{\beta}{2}$ while transmitting 2-PAM symbols. As usual, the PAM constellation with the lowest cardinality is assigned to the user with the lowest diversity order in an attempt to enhance the worst-user performance that dominates P_{sys}.

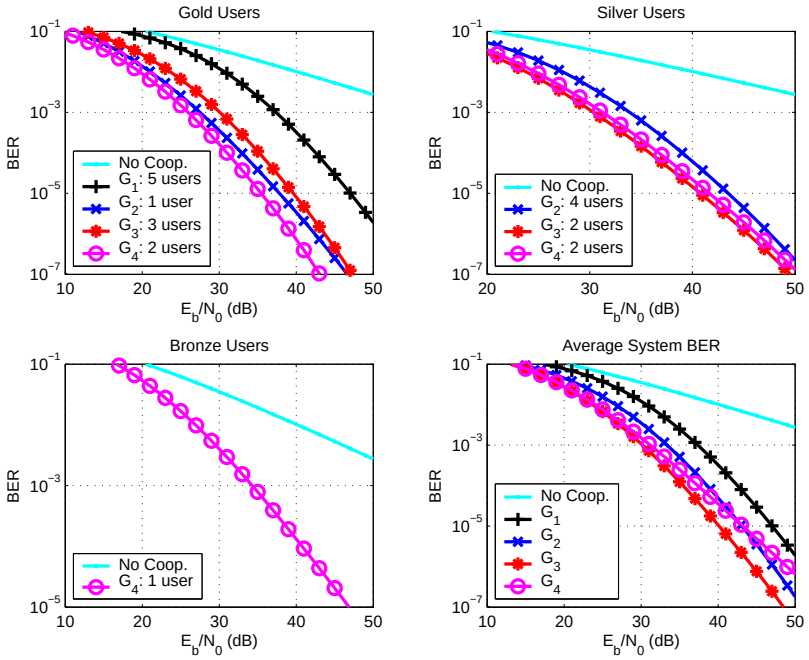

Fig. 5. Performance with $N = 5$ users. Solid and dashed lines correspond to the exact and approximate BERs, respectively. (a): gold users, (b): silver users, (c): bronze users, (d): P_{sys}.

- Grouping $G_3 = \{\{1,4\},\{2,3\}\}$ for which $\delta_{sys} = 3\frac{\beta}{2}$. For this grouping, 2 gold users profit from the diversity order 2β while the other 2 users profit from the diversity order $3\frac{\beta}{2}$. In this case, all users transmit 4-PAM symbols.

The above grouping strategies are compared in Fig. 4 for a 4 km link in the absence of pointing errors ($\varphi_1 = 4.41$, $\varphi_2 = 1.28$ and $\xi \to \infty$). Results highlight the key observation that while G_1 achieves the highest value of δ_{sys}, it manifests the worst performance for the practical SNR range below 40 dB whether in terms of the user BERs $\{P_e^{(n)}\}_{n=1}^{N}$ or in terms of the system BER P_{sys}. As explained before, this poor performance originates from the high cardinality of the 16-PAM constellation needed to embed the information from all four users. In this context, Fig. 4 shows that G_2 and G_3 constitute appealing alternatives to the all-user grouping G_1. While G_3 results in the smallest values of $P_e^{(1)}$ and $P_e^{(2)}$ (diversity order of 2β with 4-PAM), G_2 is appealing for minimizing $P_e^{(3)}$ (diversity order of 2β with 8-PAM) and $P_e^{(4)}$ (diversity order of $3\frac{\beta}{2}$ with 2-PAM). In other words, the 2 gold users of G_3 have lower BERs compared to the gold users of G_2 (Fig. 4.a) while the BERs of the 2 silver users of G_3 are higher than the BERs of the gold and silver users of G_2 (Figures 4.b and 4.c, respectively). In terms of the average system performance, Fig. 4.d shows that G_2 constitutes the best solution over the practical range of the SNR. At a BER of 10^{-4}, G_2 and G_3 outperform G_1 by 3.3 dB and 2.1 dB, respectively.

D. Cooperation with $N = 5$ Users and $N = 6$ Users

The performance of a cooperative network with 5 users is shown in Fig. 5 for a link distance of 5 km and $\omega_z/a = 10$ ($\varphi_1 = 4.92$, $\varphi_2 = 1.17$ and $\xi = 1.67$). The following groupings are compared. (i): The all-user grouping $G_1 = \{\{1,2,3,4,5\}\}$. (ii): $G_2 = \{\{4\},\{1,2,3,5\}\}$ where the simulations show that this partitioning results in 1 gold user and 4 silver users for practical values of the SNR below 50 dB. This holds despite the fact that the diversity order of the gold user (2β) is smaller than the diversity order of the silver users ($5\frac{\beta}{2}$). (iii): $G_3 = \{\{3,4\},\{1,2,5\}\}$ with 3 gold users and 2 silver users whose diversity orders are $5\frac{\beta}{2}$ and 2β, respectively. (iv): $G_4 = \{\{3\},\{2,4\},\{1,5\}\}$ where the results show that the users can be divided as 2 gold users, 2 silver users and 1 bronze user profiting from the diversity orders $5\frac{\beta}{2}$, 2β and $3\frac{\beta}{2}$, respectively.

Results in Fig. 5.a show that the 2 gold users of G_4 profit from the lowest BER followed by the 1 gold user of G_2 and the 3 gold users of G_3. In this context, for G_4, two of the users are profiting from an extremely high QoS where a performance gain of about 31 dB at a BER of 10^{-3} can be observed with respect to noncooperative transmissions. While the gold user of G_2 profits from the second best BER, the 4 silver users suffer from the highest BERs compared to the silver users of G_3 and G_4 as shown in Fig. 5.b since 16-PAM symbols are transmitted in the first case while 4-PAM symbols are transmitted in the last two cases. Even the bronze user of G_4 experiences a huge performance gain of 23 dB at 10^{-3} compared to the case of noncooperative transmissions as shown in Fig. 5.c. Regarding the average performance, Fig. 5.d shows that G_3 is the best grouping for all practical values of the SNR not exceeding 50 dB. The all-user grouping manifests the worst performance among all grouping strategies with a performance gain of 20 dB followed by G_2 with a gain of 24 dB while G_4 and G_3 attain the performance gains of 26.3 dB and 27.3 dB at a BER of 10^{-3}, respectively.

TABLE I
OPTIMAL GROUPING

N	3	4	5	6
Optimal Grouping	$\{\{2\},\{1,3\}\}$ SNR<33 dB $\{\{1,2,3\}\}$ SNR≥33 dB	$\{\{3\},\{1,2,4\}\}$	$\{\{3,4\},\{1,2,5\}\}$	$\{\{4\},\{3,5\},\{1,2,6\}\}$

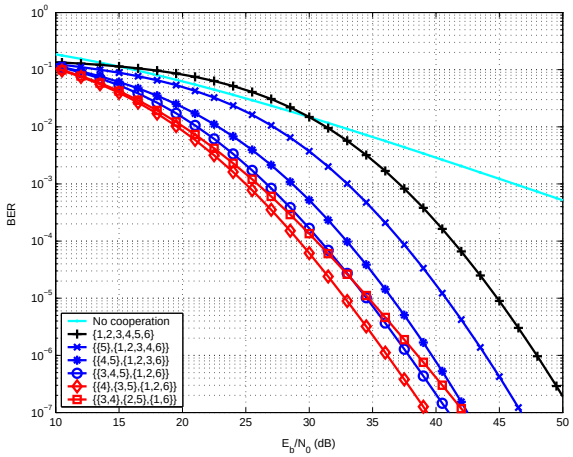

Fig. 6. Performance with $N = 6$ users for a link distance of 3 km.

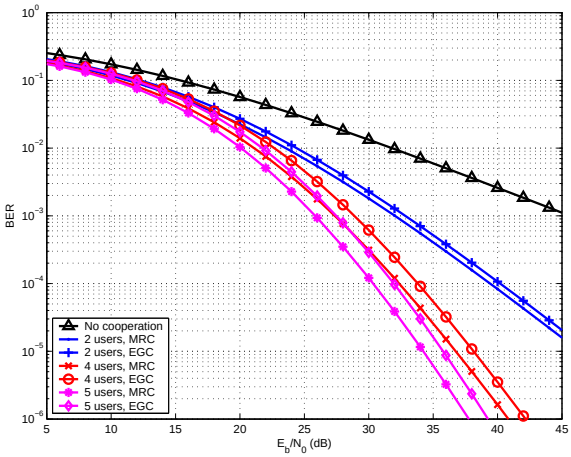

Fig. 7. Comparison between MRC and EGC for a link distance of 3 km.

While P_{sys} of G_3 and G_4 are comparable for small values of the SNR, the performance of the latter grouping deteriorates rapidly for large SNRs because of the limited diversity order of $\delta_{sys} = 3\frac{\beta}{2}$. For small SNRs, the selection among G_3 and G_4 could be based on the desired level of QoS differentiation.

Fig. 6 compares P_{sys} for different groupings with $N = 6$ users and a link distance of 3 km and $\omega_z/a = 25$ ($\varphi_1 = 4.04$, $\varphi_2 = 1.53$ and $\xi = 4.17$). Results show that the grouping $\{\{4\},\{3,5\},\{1,2,6\}\}$ achieves the best BER performance with gains of 20.5 dB and 12 dB compared to noncooperative systems and all-user grouping, respectively. This latter grouping manifests the worst performance among all grouping options and even performs worse than noncooperative transmissions for SNR values below 30 dB.

As a conclusion, the performance of the proposed scheme is highly dependent on the user grouping. The optimal groupings for different numbers of users have been determined numerically since closed-form analytical optimization is very tedious given that the pdf of the sum of n sorted channel irradiances is not known in closed-form. In some scenarios, the optimal partitioning is SNR dependent while, in other scenarios, the same partitioning ensures the optimal performance for the entire practical SNR range. The optimal groupings pertaining to the simulation setups considered in Figures 3-6 are summarized in Table I.

E. MRC versus EGC

Fig. 7 compares EGC with MRC for a link distance of 3 km in the absence of pointing errors ($\varphi_1 = 4.04$, $\varphi_2 = 1.53$ and $\xi \to \infty$). The groupings $\{\{1,2\}\}$, $\{\{3\},\{1,2,4\}\}$ and $\{\{3,4\},\{1,2,5\}\}$ are considered in the cases of 2, 4 and 5 users, respectively. In coherence with the analysis presented in Subsection IV-D, the numerical results show that EGC is capable of achieving the same diversity order as MRC where the corresponding curves are parallel to each other for large SNRs. The superiority of MRC resides in performance gains of 0.8 dB, 1.5 dB and 1.6 dB with 2, 4 and 5 users, respectively.

VI. CONCLUSION

We proposed and analyzed a novel diversity scheme for collocated multiuser FSO communications based on the concept of user grouping. The proposed solution results in very high performance gains especially for large numbers of users. In this context, enhanced diversity orders can be achieved in a cost-effective manner while avoiding any data-rate reduction and latency. Moreover, different classes of service can be created where even the worst user profits from a BER that is several orders of magnitude smaller than the BER achieved in noncooperative networks. While this scheme was considered in the context of IM/DD, it can be applied with coherent detection and subcarrier intensity modulation as well.

APPENDIX A

Based on order statistics, the joint pdf of h_i^2 and h_j^2 (with $h_i^2 \leq h_j^2$) is given by [29, 2.3.2]:

$$f_{h_i^2,h_j^2}(x,y) = \frac{N!}{(i-1)!(j-i-1)!(N-j)!} f_{h^2}(x) f_{h^2}(y) \times \left[F_{h^2}(x)\right]^{i-1} \left[F_{h^2}(y) - F_{h^2}(x)\right]^{j-i-1} \left[1 - F_{h^2}(y)\right]^{N-j}, \quad (35)$$

where $0 \leq x \leq y$.

Replacing the pdf and cdf of h^2 by the approximate expressions given in (9)-(10) and applying the binomial expansion, (35) can be written as ($0 \leq x \leq y$):

$$f_{h_i^2,h_j^2}(x,y) = \sum_{m=0}^{j-i-1} \sum_{m'=0}^{N-j} c_{m,m'} x^{\frac{\beta}{2}(j-1-m)-1} y^{\frac{\beta}{2}(m+m'+1)-1}, \quad (36)$$

where $c_{m,m'}$ is a constant term given by:

$$c_{m,m'} = \frac{N!}{4(i-1)!(j-i-1)!(N-j)!} a^j \beta^{2-j} \binom{j-i-1}{m} \binom{N-j}{m'} (-1)^{j-i-1-m+m'} \left(\frac{a}{\beta}\right)^{m'}. \quad (37)$$

The cdf of the r.v. $h_i^2 + h_j^2$ can be calculated from:

$$F_{h_i^2+h_j^2}(h) = \Pr(h_i^2 + h_j^2 \leq h) = \int_0^{\frac{h}{2}} \int_x^{h-x} f_{h_i^2,h_j^2}(x,y) \mathrm{d}y \mathrm{d}x, \quad (38)$$

where the boundaries of the double integral follow from the inequalities $0 \leq h_i^2 \leq h_j^2$ and $h_i^2 + h_j^2 \leq h$.

In order to evaluate the pdf $f_{h_i^2+h_j^2}(h) = \frac{\mathrm{d}}{\mathrm{d}h}[F_{h_i^2+h_j^2}(h)]$, the Leibniz integral rule is applied twice on the functions $\int_x^{h-x} f_{h_i^2,h_j^2}(x,y)\mathrm{d}y$ and $f_{h_i^2,h_j^2}(x,y)$ resulting in the following expression:

$$f_{h_i^2+h_j^2}(h) = \int_0^{\frac{h}{2}} f_{h_i^2,h_j^2}(x,h-x)\mathrm{d}x \quad (39)$$

$$= \sum_{m=0}^{j-i-1} \sum_{m'=0}^{N-j} c_{m,m'} \int_0^{\frac{h}{2}} x^{\frac{\beta}{2}(j-1-m)-1} (h-x)^{\frac{\beta}{2}(m+m'+1)-1} \mathrm{d}x. \quad (40)$$

Performing the change of variable $u = \frac{x}{h}$ and solving the obtained integral results in:

$$f_{h_i^2+h_j^2}(h) = \sum_{m=0}^{j-i-1} \sum_{m'=0}^{N-j} c_{m,m'} \times B\left(\frac{1}{2}; \frac{\beta}{2}(j-m-1), \frac{\beta}{2}(m+m'+1)\right) h^{\frac{\beta}{2}(j+m')-1}. \quad (41)$$

The dominant term in (41) for small values of h corresponds to $m' = 0$. Replacing $m' = 0$ in (41) and simplifying the answer results in the expression given in (25).

Appendix B

Based on order statistics, the joint pdf of the three r.v.s h_i^2, h_j^2 and h_k^2 (with $h_i^2 \leq h_j^2 \leq h_k^2$) is given by [29, 2.4.7]:

$$f_{h_i^2,h_j^2,h_k^2}(x,y,z) = \frac{N!}{(i-1)!(j-i-1)!(k-j-1)!(N-k)!} f_{h_i^2}(x) f_{h_j^2}(y) f_{h_k^2}(z) \left[F_{h_i^2}(x)\right]^{i-1} \left[F_{h_j^2}(y) - F_{h_i^2}(x)\right]^{j-i-1} \left[F_{h_k^2}(z) - F_{h_j^2}(y)\right]^{k-j-1} \left[1 - F_{h_k^2}(z)\right]^{N-k}, \quad (42)$$

where $0 \leq x \leq y \leq z$.

Replacing the pdf and cdf of h^2 by the approximate expressions given in (9)-(10) and applying the binomial expansion, (42) can be written as ($0 \leq x \leq y \leq z$):

$$f_{h_i^2,h_j^2,h_k^2}(x,y,z) = \sum_{m=0}^{j-i-1} \sum_{m'=0}^{k-j-1} \sum_{m''=0}^{N-k} c_{m,m',m''} \times x^{\frac{\beta}{2}(j-m-1)-1} y^{\frac{\beta}{2}(k-j+m-m')-1} z^{\frac{\beta}{2}(m'+m''+1)-1}, \quad (43)$$

where:

$$c_{m,m',m''} \triangleq \frac{N!}{8(i-1)!(j-i-1)!(k-j-1)!(N-k)!} a^k \beta^{3-k} \binom{j-i-1}{m} \binom{k-j-1}{m'} \binom{N-k}{m''} (-1)^{k-i-m-m'+m''} \left(\frac{a}{\beta}\right)^{m''}. \quad (44)$$

The cdf of the r.v. $h_i^2 + h_j^2 + h_k^2$ can be written as follows:

$$F_{h_i^2+h_j^2+h_k^2}(h) = \Pr\left(h_i^2 + h_j^2 + h_k^2 \leq h\right) = \int_0^{\frac{h}{3}} \int_x^{\frac{h-x}{2}} \int_y^{h-x-y} f_{h_i^2,h_j^2,h_k^2}(x,y,z) \mathrm{d}z \mathrm{d}y \mathrm{d}x, \quad (45)$$

where the boundaries of the integrals follow from $0 \leq x \leq y \leq z$ and $x + y + z \leq h$.

Differentiating (45) with respect to h by applying the Leibniz integral rule results in the following expression of the pdf:

$$f_{h_i^2+h_j^2+h_k^2}(h) = \int_0^{\frac{h}{3}} \int_x^{\frac{h-x}{2}} f_{h_i^2,h_j^2,h_k^2}(x,y,h-x-y) \mathrm{d}y \mathrm{d}x. \quad (46)$$

Replacing (43) in (46) and solving the integral with respect to y by performing the change of variable $u = \frac{y}{h-x}$ results in the following expression:

$$f_{h_i^2+h_j^2+h_k^2}(h) = \sum_{m,m',m''} c_{m,m',m''} \int_0^{\frac{h}{3}} x^{\frac{\beta}{2}(j-m-1)-1} (h-x)^{\frac{\beta}{2}(k-j+m+m''+1)-1} \times \left[B\left(\frac{1}{2}; (k-j+m-m')\frac{\beta}{2}, (m'+m''+1)\frac{\beta}{2}\right) - B\left(\frac{x}{h-x}; (k-j+m-m')\frac{\beta}{2}, (m'+m''+1)\frac{\beta}{2}\right)\right] \mathrm{d}x. \quad (47)$$

Eq. (47) can be further split into two integrals. While the first one can be readily expressed in terms of the incomplete beta function, the second integral (involving the term $B\left(\frac{x}{h-x}; .,.\right)$) can not be solved in closed-form. Applying the series expansion $B(z;a,b) = z^a \sum_{r=0}^{+\infty} \frac{(1-b)_r}{(a+r)r!} z^r$ [30] and solving the obtained integrals by performing the change of variable $u = \frac{x}{h}$ results in:

$$f_{h_i^2+h_j^2+h_k^2}(h) = \sum_{m,m',m''} c_{m,m',m''} h^{(k+m'')\frac{\beta}{2}-1} \times \left[B\left(\frac{1}{2}; (k-j+m-m')\frac{\beta}{2}, (m'+m''+1)\frac{\beta}{2}\right) B\left(\frac{1}{3}; (j-m-1)\frac{\beta}{2}, (k-j+m+m''+1)\frac{\beta}{2}\right) - \sum_{r=0}^{+\infty} \frac{\left[1-(m'+m''+1)\frac{\beta}{2}\right]_r}{\left((k-j+m-m')\frac{\beta}{2}+r\right) r!} B\left(\frac{1}{3}; (k-m'-1)\frac{\beta}{2}+r, (m'+m''+1)\frac{\beta}{2}-r\right)\right]. \quad (48)$$

The dominant term in the power series expansion provided in (48) corresponds to $m'' = 0$. Replacing m'' by 0 in (48) results in the expressions given in (26)-(27).

APPENDIX C

For simplicity of notation, we set $n = N_{\mathcal{S}}$ in this appendix. Based on order statistics, the joint pdf of the n r.v.s $h_{i_1}^2, \ldots, h_{i_n}^2$ (with $h_{i_1}^2 \leq \cdots \leq h_{i_n}^2$) can be written as [31]:

$$f_{h_{i_1}^2,\ldots,h_{i_n}^2}(x_1,\ldots,x_n) = N! \prod_{j=1}^{n} f_{h_j^2}(x_j) \prod_{j=0}^{n} \frac{\left[F_{h_{j+1}^2}(x_{j+1}) - F_{h_j^2}(x_j)\right]^{i_{j+1}-i_j-1}}{(i_{j+1}-i_j-1)!}, \quad (49)$$

where $0 \leq x_1 \leq \cdots \leq x_n$, $i_0 \triangleq 0$, $i_{n+1} \triangleq N+1$, $x_0 \triangleq -\infty$ and $x_{n+1} \triangleq +\infty$.

Replacing the pdf's and cdf's of the constituent r.v.s by their approximate expressions in (9)-(10) and applying the binomial expansion on the terms $\left[F_{h_{j+1}^2}(x_{j+1}) - F_{h_j^2}(x_j)\right]^{i_{j+1}-i_j-1}$ for $j = 1, \ldots, n$ results in:

$$f_{h_{i_1}^2,\ldots,h_{i_n}^2}(x_1,\ldots,x_n) = \sum_{m_1=0}^{i_2-i_1-1} \cdots \sum_{m_{n-1}=0}^{i_n-i_{n-1}-1} \sum_{m_n=0}^{N-i_n} c_{m_1,\ldots,m_n} \prod_{j=1}^{n} x_j^{P_j-1} \quad ; \quad 0 \leq x_1 \leq \cdots \leq x_n, \quad (50)$$

where $c_{m_1,\ldots,m_n}$ is a constant that is given by:

$$c_{m_1,\ldots,m_n} = \frac{N!}{2^n (i_1-1)!} a^{i_n+m_n} \beta^{n-i_n-m_n} (-1)^{i_n-i_1-(n-1)+m_n-\sum_{j=1}^{n-1} m_j} \prod_{j=1}^{n} \frac{\binom{i_{j+1}-i_j-1}{m_j}}{(i_{j+1}-i_j-1)!}. \quad (51)$$

In (50), it is straightforward to prove that the powers $\{P_j\}_{j=1}^n$ can be calculated as follows:

$$P_j = \begin{cases} \frac{\beta}{2}(i_2 - 1 - m_1), & j = 1; \\ \frac{\beta}{2}(i_{j+1} - i_j + m_{j-1} - m_j), & j = 2, \ldots, n-1; \\ \frac{\beta}{2}(1 + m_{n-1} + m_n), & j = n. \end{cases} \quad (52)$$

The next step in our calculations corresponds to deriving the cdf $F_{\sum_{j=1}^n h_{i_j}^2}(h) = \Pr\left(\sum_{j=1}^n h_{i_j}^2 \leq h\right)$ where the derivations must take into account the inequalities $0 \leq x_1 \leq \cdots \leq x_n$ and $x_1 + \cdots + x_n \leq h$. Inspecting the variable x_k shows that this variable must satisfy the $n-k$ inequalities $x_k \leq x_{k+1}$, $x_k \leq x_{k+2}$, $\cdots$ $x_k \leq x_n$ as well as the inequality $x_k + (x_{k+1} + \cdots x_n) \leq h - \sum_{j=1}^{k-1} x_j$. Adding the above inequalities results in the following boundaries of the integral over x_k:

$$x_k \in \left[x_{k-1} \quad \frac{h - \sum_{j=1}^{k-1} x_j}{n-k+1}\right] \quad ; \quad k = 1, \ldots, n \ , \ x_0 \triangleq 0. \quad (53)$$

Based on (50) and (53), the approximate cdf of the r.v. $\sum_{j=1}^n h_{i_j}^2$ can be evaluated by solving the n integrals:

$$F_{\sum_{j=1}^n h_{i_j}^2}(h) = \sum_{m_1,\ldots,m_n} c_{m_1,\ldots,m_n} \int_0^{\frac{h}{n}} x_1^{P_1-1} \int_{x_1}^{\frac{h-x_1}{n-1}} x_2^{P_2-1} \cdots \int_{x_{n-2}}^{\frac{h-\sum_{j=1}^{n-2} x_j}{2}} x_{n-1}^{P_{n-1}-1} \int_{x_{n-1}}^{h-\sum_{j=1}^{n-1} x_j} x_n^{P_n-1} \mathrm{d}x_n \cdots \mathrm{d}x_1. \quad (54)$$

Differentiating (54) with respect to h reduces the n integrals to $n-1$ integrals resulting in the following expression of the pdf of $\sum_{j=1}^n h_{i_j}^2$:

$$f_{\sum_{j=1}^n h_{i_j}^2}(h) = \sum_{m_1,\ldots,m_n} c_{m_1,\ldots,m_n} \int_0^{\frac{h}{n}} x_1^{P_1-1} \cdots \int_{x_{n-2}}^{\frac{h-\sum_{j=1}^{n-2} x_j}{2}} x_{n-1}^{P_{n-1}-1} \left(h - \sum_{j=1}^{n-1} x_j\right)^{P_n-1} \mathrm{d}x_{n-1} \cdots \mathrm{d}x_1, \quad (55)$$

where the Leibniz integral rule was invoked.

The integrals in (55) are not separable since the boundaries contain the variables $x_1, \ldots, x_{n-2}$. The solution of the involved integrals will be provided in what follows.

Proposition 5: The successive solution of the integrals with respect to x_{n-1}, x_{n-2} reaching x_1 shows that the integral with respect to x_{n-k} (for $k = 1, \ldots, n-1$) can be written under the following general form:

$$\mathfrak{I}_{n-k} = \sum_{r_1 \in \mathcal{R}_1} \cdots \sum_{r_{k-1} \in \mathcal{R}_{k-1}} \xi_{r_1} \cdots \xi_{r_{k-1}} \int_{x_{n-(k+1)}}^{\frac{h-\sum_{j=0}^{n-(k+1)} x_j}{k+1}} x_{n-k}^{P_{n-k}-1} x_{n-k}^{\sum_{k'=1}^{k-1}(P_{n-k'}+r_{k'})} \left(h - \sum_{j=1}^{n-k} x_j\right)^{P_n - \sum_{k'=1}^{k-1} r_{k'} - 1} \mathrm{d}x_{n-k}, \quad (56)$$

where the constants $\{\xi_{r_k}\}_{k=1}^{n-2}$ are determined recursively according to the relation ($k = 1, \ldots, n-2$):

$$\xi_{r_k} = \begin{cases} B\left(\frac{1}{k+1}; \sum_{k'=1}^{k} P_{n-k'} + \sum_{k'=1}^{k-1} r_{k'}, P_n - \sum_{k'=1}^{k-1} r_{k'}\right); \\ -\frac{\left(1-P_n+\sum_{k'=1}^{k-1} r_{k'}\right)_{r_k}}{\left(\sum_{k'=1}^{k} P_{n-k'} + \sum_{k'=1}^{k-1} r_{k'} + r_k\right) r_k!}. \end{cases} \quad (57)$$

where the first expression holds in the case $r_k < 0$ while the second expression holds in the case $r_k \geq 0$.

and where each one of the sets $\mathcal{R}_1, \ldots, \mathcal{R}_{n-2}$ comprises one negative integer and an infinite number of positive integers as follows:

$$\mathcal{R}_k = \left\{ -\sum_{k'=1}^{k} P_{n-k'} - \sum_{k'=1}^{k-1} r_{k'} \right\} \cup \mathbb{N} \quad ; \quad k = 1, \ldots, n-2, \quad (58)$$

where $\mathbb{N}$ stands for the set of natural integers.

Proof: First of all, the boundaries of the integral in (56) follow directly from (53) by replacing k by $n-k$.

The relations (56), (57) and (58) will be proven by induction. First, we will prove that the relations hold for $k=1$. In this case, from (55), the integral with respect to x_{n-1} is equal to:

$$\mathfrak{I}_{n-1} = \int_{x_{n-2}}^{\frac{h-\sum_{j=1}^{n-2} x_j}{2}} x_{n-1}^{P_{n-1}-1} \left(h - \sum_{j=1}^{n-1} x_j \right)^{P_n-1} \mathrm{d}x_{n-1}, \tag{59}$$

which corresponds to the general form provided in (56) for $k=1$.

Next, we assume that (56) holds for k and we prove that it will hold for $k+1$. Performing the change of variable $u = \frac{x_{n-k}}{h-\sum_{k'=1}^{n-(k+1)} x_j}$, (56) can be written as:

$$\mathfrak{I}_{n-k} = \sum_{r_1,\ldots,r_{k-1}} \xi_{r_1} \cdots \xi_{r_{k-1}} \left(h - \sum_{j=1}^{n-(k+1)} x_j \right)^{P_n+\sum_{k'=1}^{k} P_{n-k'}-1} \int_{\frac{x_{n-(k+1)}}{h-\sum_{k'=1}^{n-(k+1)} x_j}}^{\frac{1}{k+1}} u^{A_k-1} (1-u)^{B_k-1} \mathrm{d}x_{n-k}, \tag{60}$$

where:

$$A_k \triangleq \sum_{k'=1}^{k} P_{n-k'} + \sum_{k'=1}^{k-1} r_{k'} \quad ; \quad B_k \triangleq P_n - \sum_{k'=1}^{k-1} r_{k'}. \tag{61}$$

The integral in (60) can be readily solved in terms of the incomplete beta function:

$$\mathfrak{I}_{n-k} = \sum_{r_1 \in \mathcal{R}_1} \cdots \sum_{r_{k-1} \in \mathcal{R}_{k-1}} \xi_{r_1} \cdots \xi_{r_{k-1}} \left(h - \sum_{j=1}^{n-(k+1)} x_j \right)^{P_n+\sum_{k'=1}^{k} P_{n-k'}-1} \left[B\left(\frac{1}{k+1}; A_k, B_k \right) - B\left(\frac{x_{n-(k+1)}}{h-\sum_{k'=1}^{n-(k+1)} x_j}; A_k, B_k \right) \right]. \tag{62}$$

Since the second incomplete beta function in (62) will lead to integrals with respect to $x_{n-(k+1)}, \ldots, x_1$ that can not be solved, we apply the series expansion $B(z;a,b) = z^a \sum_{r=0}^{+\infty} \frac{(1-b)_r}{(a+r)r!} z^s$ on this function [30]. Considering the first incomplete beta function in (62) (which is a constant) as a special term in the expansion, (62) can be written in a compact form as:

$$\mathfrak{I}_{n-k} = \sum_{r_1 \in \mathcal{R}_1} \cdots \sum_{r_{k-1} \in \mathcal{R}_{k-1}} \sum_{r_k \in \mathcal{X}} \xi_{r_1} \cdots \xi_{r_{k-1}} \zeta \; x_{n-(k+1)}^{A_k+r_k} \left(h - \sum_{j=1}^{n-(k+1)} x_j \right)^{P_n+\sum_{k'=1}^{k} P_{n-k'}-A_k-r_k-1} \tag{63}$$

In (63), $\mathcal{X} = \{-A_k\} \cup \mathbb{N}$ and $\zeta = B\left(\frac{1}{k+1}; A_k, B_k\right)$ if $r_k = -A_k$ and $\zeta = -\frac{[1-B_k]_{r_k}}{(A_k+r_k)r_k!}$ otherwise. Replacing A_k and B_k by their values from (61) shows that $\mathcal{X}$ is equal to the set $\mathcal{R}_k$ given in (58) while the constant ζ is equal to the ξ_{r_k} defined in (57). Finally, in order to find $\mathfrak{I}_{n-(k+1)}$, (63) must be multiplied by $x_{n-(k+1)}^{P_{n-(k+1)}-1}$ following from the pdf expression in (50). Carrying out this multiplication while replacing A_k and B_k by their values from (61) shows that (63) can be obtained from (56) by replacing k with $k+1$ completing the proof. ∎

Based on the approach presented in proposition 5, the pdf in (55) can be written as $f_{\sum_{j=1}^{n} h_{i_j}^2}(h) = \sum_{m_1,\ldots,m_n} c_{m_1,\ldots,m_n} \mathfrak{I}_1$. Setting $k = n-1$ in (56) results in:

$$\begin{aligned} \mathfrak{I}_1 &= \sum_{r_1 \in \mathcal{R}_1} \cdots \sum_{r_{n-2} \in \mathcal{R}_{n-2}} \xi_{r_1} \cdots \xi_{r_{n-2}} \int_0^{\frac{h}{n}} x_1^{P_1-1} x_1^{\sum_{k'=1}^{n-2}(P_{n-k'}+r_{k'})} (h-x_1)^{P_n-\sum_{k'=1}^{n-2} r_{k'}-1} \mathrm{d}x_1 \\ &= h^{\sum_{k'=0}^{n-1} P_{n-k'}-1} \left[\sum_{r_1 \in \mathcal{R}_1} \cdots \sum_{r_{n-2} \in \mathcal{R}_{n-2}} \xi_{r_1} \cdots \xi_{r_{n-2}} B\left(\frac{1}{n}; \sum_{k'=1}^{n-1} P_{n-k'} + \sum_{k'=1}^{n-2} r_{k'}, P_n - \sum_{k'=1}^{n-2} r_{k'} \right) \right]. \end{aligned} \tag{64}$$

In (64), the power of h is $\sum_{k'=0}^{n-1} P_{n-k'} - 1 = \sum_{j=1}^{N} P_j - 1 = \frac{\beta}{2}(i_n + m_n) - 1$ following from (52). As a conclusion, the dominant term in $f_{\sum_{j=1}^{n} h_{i_j}^2}(h) = \sum_{m_1,\ldots,m_n} c_{m_1,\ldots,m_n} \mathfrak{I}_1$ corresponds to $m_n = 0$. Replacing m_n by 0 in (51), equations (29)-(33) follow from (52), (57), (58) and (64).

REFERENCES

[1] X. Tang, Z. Xu, and Z. Ghassemlooy, "Coherent polarization modulated transmission through MIMO atmospheric optical turbulence channel," *J. Lightwave Technol.*, vol. 31, no. 20, pp. 3221–3228, Oct. 2013.

[2] P. Wang, L. Zhang, L. Guo, F. Huang, T. Shang, R. Wang, and Y. Yang, "Average BER of subcarrier intensity modulated free space optical systems over the exponentiated Weibull fading channels," *Optics Express*, vol. 22, no. 17, pp. 20 828–20 841, Aug. 2014.

[3] S. M. Aghajanzadeh and M. Uysal, "Multi-hop coherent free-space optical communications over atmospheric turbulence channels," *IEEE Trans. Commun.*, vol. 59, no. 6, pp. 1657 – 1663, June 2011.

[4] S. Kazemlou, S. Hranilovic, and S. Kumar, "All-optical multihop free-space optical communication systems," *J. Lightwave Technol.*, vol. 29, no. 18, pp. 2663 – 2669, Sep. 2011.

[5] M. Safari and M. Uysal, "Relay-assisted free-space optical communication," *IEEE Trans. Wireless Commun.*, vol. 7, no. 12, pp. 5441 – 5449, Dec. 2008.

[6] M. Karimi and M. Nasiri-Kenari, "Free-space optical communications via optical amplify-and-forward relaying," *J. Lightwave Technol.*, vol. 29, no. 2, pp. 242–2248, Jan. 2011.

[7] J. Park, E. Lee, C.-B. Chae, and G. Yoon, "Outage probability analysis of a coherent FSO amplify-and-forward relaying system," *IEEE Photon. Technol. Lett.*, vol. 27, no. 11, pp. 1204–1207, June 2015.

[8] M. R. Bhatnagar, "Performance analysis of decode-and-forward relaying in gamma-gamma fading channels," *IEEE Photon. Technol. Lett.*, vol. 24, no. 7, pp. 545 – 547, April 2012.

[9] S. Aghajanzadeh and M. Uysal, "Outage performance and DMT analysis of DF parallel relaying in FSO IM/DD communications," in *IEEE Vehicular Technol. Conference*, Québec Canada, Sep. 2012, pp. 1 – 5.

[10] M. Aggarwal, P. Garg, and P. Puri, "Analysis of subcarrier intensity modulation-based optical wireless DF relaying over turbulence channels with path loss and pointing error impairments," *IET Commun.*, vol. 8, no. 17, pp. 3170–3178, July 2014.

[11] N. D. Chatzidiamantis, D. S. Michalopoulos, E. E. Kriezis, G. K. Karagiannidis, and R. Schober, "Relay selection protocols for relay-assisted free-space optical systems," *IEEE J. Opt. Commun. Netw.*, vol. 5, no. 1, pp. 4790 –4807, Jan. 2013.

[12] C. Abou-Rjeily, "Performance analysis of selective relaying in cooperative free-space optical systems," *J. Lightwave Technol.*, vol. 31, no. 18, pp. 2965–2973, Sep. 2013.

[13] ——, "All-active and selective FSO relaying: Do we need inter-relay cooperation?" *J. Lightwave Technol.*, vol. 32, no. 10, pp. 1899 – 1906, May 2014.

[14] C. Abou-Rjeily and S. Haddad, "Inter-relay cooperation: A new paradigm for enhanced relay-assisted FSO communications," *IEEE Trans. Commun.*, vol. 62, no. 6, pp. 1970 – 1982, June 2014.

[15] S. Yang and J.-C. Belfiore, "Optimal space-time codes for the MIMO amplify-and-forward cooperative channel," *IEEE Trans. Inform. Theory*, vol. 53, no. 2, pp. 647–663, February 2007.

[16] B. Zhu, J. Cheng, M. Alouini, and L. Wu, "Relay placement for FSO multi-hop DF systems with link obstacles and infeasible regions," *IEEE Trans. Wireless Commun.*, vol. 14, no. 9, pp. 5240 – 5250, Sep. 2015.

[17] J. Abouei and K. N. Plataniotis, "Multiuser diversity scheduling in free-space optical communications," *J. Lightwave Technol.*, vol. 30, no. 9, pp. 1351–1358, May 2012.

[18] L. Yang, X. Gao, and M.-S. Alouini, "Performance analysis of free-space optical communication systems with multiuser diversity over atmospheric turbulence channels," *IEEE Photonics Journal*, vol. 6, no. 2, pp. 1–17, April 2014.

[19] P. Wang, N. Xiang, Q. Gao, R. Wang, L. Guo, and Y. Yang, "On the performances of N-th best user selection scheme in multiuser diversity free-space optical systems over exponentiated Weibull turbulence channels," *IEEE Photonics Journal*, vol. 8, no. 2, pp. 1–15, April 2016.

[20] S. Zhalehpour, M. Uysal, O. A. Dobre, and T. Ngatched, "Outage capacity and throughput analysis of multiuser FSO systems," in *Proc. IEEE Canadian Workshop on Inf. Theory*, St. John's NL Canada, July 2015, pp. 143 – 146.

[21] S. Zhalehpour and M. Uysal, "Performance of multiuser scheduling in free space optical systems over atmospheric turbulence channels," *IET Optoelectronics*, vol. 9, no. 5, pp. 275–281, April 2015.

[22] P. Puri, P. Garg, and M. Aggarwal, "Multiple user pair scheduling in TWR assisted FSO systems," *IEEE J. Opt. Commun. Netw.*, vol. 8, no. 5, pp. 290–301, May 2016.

[23] M. Safari and M. Uysal, "Do we really need OSTBCs for free-space optical communication with direct detection?" *IEEE Trans. Wireless Commun.*, vol. 7, no. 11, pp. 4445 – 4448, Nov. 2008.

[24] C. Abou-Rjeily, "On the optimality of the selection transmit diversity for MIMO-FSO links with feedback," *IEEE Commun. Lett.*, vol. 15, no. 6, pp. 641 – 643, June 2011.

[25] D. G. Brennan, "Linear diversity combining techniques," in *Proc. of the IEEE*, vol. 91, no. 2, Feb. 2003, pp. 331–356.

[26] H. Sandalidis, T. Tsiftsis, and G. Karagiannidis, "Optical wireless communications with heterodyne detection over turbulence channels with pointing errors," *J. Lightwave Technol.*, vol. 27, no. 20, pp. 4440–4445, October 2009.

[27] R. Boluda-Ruiz, A. Garcia-Zambrana, C. Castillo-Vasquez, and B. Castillo-Vasquez, "Adaptive selective relaying in cooperative free-space optical systems over atmospheric turbulence and misalignment fading channels," *Opt. Express*, vol. 22, no. 13, pp. 16 629 – 16 644, June 2014.

[28] C. Aboy-Rjeily, "Diversity orders and coding gains of repetition coding and transmit laser selection over MIMO free-space optical links," in *Proc. IEEE Int. Symp. on Wireless Commun. Systems*, Barcelona Spain, Aug. 2014, pp. 90 – 94.

[29] B. C. Arnold, N. Balakrishnan, and H. N. Nagaraja, *A First Course in Order Statistics*. Wiley, 1992.

[30] Wolfram mathworld. [Online]. Available: http://mathworld.wolfram.com/IncompleteBetaFunction.html.

[31] P. N. Chen. Basic theories on order statistics. [Online]. Available: http://shannon.cm.nctu.edu.tw/prob/OR2s08.pdf